

Medium Modifications and Production of Charmonia at LHC

Xingbo Zhao¹ and Ralf Rapp²

¹ *Department of Physics and Astronomy, Iowa State University, Ames, Iowa 50011, USA*

² *Cyclotron Institute and Department of Physics and Astronomy,
Texas A&M University, College Station, TX 77843-3366, USA*

(Dated: February 16, 2022)

A previously constructed transport approach to calculate the evolution of quarkonium yields and spectra in heavy-ion collisions is applied to Pb-Pb($\sqrt{s}=2.76$ ATeV) collisions at the Large Hadron Collider (LHC). In this approach spectral properties of charmonia are constrained by euclidean correlators from thermal lattice QCD and subsequently implemented into a Boltzmann equation accounting for both suppression and regeneration reactions. Based on a fair description of SPS and RHIC data, we provide predictions for the centrality dependence of J/ψ yields at LHC. The main uncertainty is associated with the input charm cross section, in particular its hitherto unknown reduction due to shadowing in nuclear collisions. Incomplete charm-quark thermalization and non-equilibrium in charmonium chemistry entail a marked reduction of the regeneration yield compared to the statistical equilibrium limit.

PACS numbers: 25.75.-q, 12.38.Mh, 14.40.Pq

I. INTRODUCTION

In recent years it has been realized that early ideas of associating charmonium suppression in ultrarelativistic heavy-ion collisions (URHICs) with the deconfinement transition [1] are less direct than originally hoped for, see Refs. [2–4] for recent reviews. While there is little doubt that a sufficiently hot and dense medium created in URHICs induces a large suppression of primordially (or would-be) produced charmonia, coalescence processes of charm and anti-charm quarks in the later stages of the medium evolution are now believed to play an important role in a quantitative description of charmonium observables. The regeneration reactions are, in fact, dictated by the principle of detailed balance and are operative once a charmonium bound state can be supported in the heat bath [5–11]. The onset of regeneration for each charmonium state in the cooling process of the bulk matter is thus dictated by its “dissociation temperature”, T_{diss}^{Ψ} , which in general will be different for ground ($\Psi=\eta_c, J/\psi$) and excited states ($\Psi=\psi', \chi_c$, etc.). Furthermore, the inelastic reaction rate, Γ_{Ψ} , of each charmonium controls its approach to the equilibrium limit. Both reaction rate (inelastic width) and equilibrium limit depend on the temperature and thus change as the system evolves in a heavy-ion reaction. The balance between primordially produced and regenerated charmonia can therefore be expected to be sensitive to the spectral properties of charmonia in the Quark-Gluon Plasma (QGP).

In Ref. [12] we have implemented basic properties of charmonium spectral functions (mass, width and binding energy) into a Boltzmann transport equation. The spectral properties have been estimated from an in-medium potential model [13] and checked against euclidean correlators from thermal lattice QCD. Since the definition of an in-medium two-body heavy-quark potential remains an open problem to date, we have investigated two limit-

ing cases representing a “weak-binding scenario” (WBS) and a “strong-binding scenario” (SBS) which are characterized by a small ($1.2T_c$) and large ($2T_c$) J/ψ dissociation temperature, respectively. The corresponding phenomenological analysis of J/ψ production in URHICs at SPS ($\sqrt{s}=17.3$ AGeV) and RHIC ($\sqrt{s}=200$ AGeV), solving a rate equation in a thermally expanding fireball background, revealed that both SBS and WBS can be compatible with currently available data, despite the factor of ~ 10 difference in collision energy. The key difference is the *composition* of the final yield, especially in central A-A collisions, where the regeneration (primordial) component is much larger in the WBS (SBS) than in the SBS (WBS). However, since the individual excitation functions (\sqrt{s} dependence) of the primordial and regenerated components are quite opposite (decreasing vs. increasing, respectively) [14], it is hoped that another factor of ~ 10 increase in collision energy is able to disentangle at least the two limiting scenarios. An initial investigation of this possibility is the main purpose of this paper, by providing predictions for inclusive J/ψ production in Pb-Pb collisions at $\sqrt{s}=2760$ AGeV as recently conducted at the Large Hadron Collider (LHC). Another important point is in how far chemical and thermal off-equilibrium effects cause a deviation from the equilibrium limit as predicted, e.g., in the statistical hadronization model [15, 16].

The main uncertainty in our predictions will be associated with the input for the open-charm cross section (as well as its shadowing in Pb-Pb). Here, preliminary LHC data from p - p collisions will be utilized in connection with theoretical estimates for shadowing effects. The charged particle multiplicity, dN_{ch}/dy , has already been measured and will be used to constrain the total entropy in the system at each centrality. The total multiplicity is not only important for the initial temperature and its evolution but also determines the volume of the system

at given temperature which affects the charm-quark density (for given total number of charm pairs, $N_{c\bar{c}}$) and thus the equilibrium limit of charmonia.

In the following we first recapitulate our framework for calculating the evolution of charmonia in URHICs and the connection to their spectral properties (Sec. II), discuss the open- and hidden-charm input quantities for Pb-Pb at $\sqrt{s}=2760$ AGeV (Sec. III), evaluate results for the centrality dependence of inclusive J/ψ yields (Sec. IV) and conclude (Sec. V).

II. RATE EQUATION AND SPECTRAL PROPERTIES OF CHARMONIA

In this section we briefly recall the main features of constructing the equilibrium properties of charmonia ($\Psi=J/\psi$, χ_c and ψ') in the Quark-Gluon Plasma (QGP) and hadron gas (HG), and their implementation into a thermal rate equation following Ref. [12] (which contains a more detailed account of our approach). Upon integrating over the spatial and momentum dependence of the Boltzmann equation one arrives at a simplified (averaged) rate equation for the number, $N_\Psi(\tau)$, of state Ψ in a heavy-ion collision,

$$\frac{dN_\Psi}{d\tau} = -\Gamma_\Psi(T) [N_\Psi - N_\Psi^{\text{eq}}(T)] . \quad (1)$$

The dissociation (and formation) rate, Γ_Ψ , is computed in the so-called quasifree approximation for the processes $p + \Psi \rightarrow p + c + \bar{c}$ induced by light partons, p , of the heat bath (u , d , s anti-/quarks and gluons) [14]. Besides the trivial T dependence induced by the number density of the light partons, the charmonium binding energy,

$$\varepsilon_B(T) = 2m_c^*(T) - m_\Psi(T) , \quad (2)$$

plays an important in that states with larger ε_B are characterized by a smaller $\Gamma_\Psi(T)$; this ensures a realistic hierarchy between ground and excited states, and is responsible for the main difference in $\Gamma_\Psi(T)$ between the SBS and WBS. The binding energies, $\varepsilon_B(T)$, in these two scenarios are taken from T -matrix calculations [13] using lQCD results for either the internal ($U_{Q\bar{Q}}(r; T)$) or free energy ($F_{Q\bar{Q}}(r; T)$) as interaction potential, respectively. Within each scenario the in-medium charm-quark mass is fixed according to $2m_c^*(T) = U_{Q\bar{Q}}(\infty; T)$ or $F_{Q\bar{Q}}(\infty; T)$, which also determines the charmonium mass, $m_\Psi(T)$, via Eq. (2). The latter figures into the statistical equilibrium limit of each state,

$$N_\Psi^{\text{stat}}(T) = \gamma_c^2(N_{c\bar{c}}; T) V_{\text{FB}} d_\Psi \int \frac{d^3p}{(2\pi)^3} f^\Psi(p; T) , \quad (3)$$

where d_Ψ denotes the spin degeneracy, $f^\Psi(p; T)$ the Bose distribution and V_{FB} the (time-dependent) fireball volume. The charm-quark fugacity, $\gamma_c(T) = \gamma_{\bar{c}}(T)$, is determined by assuming a fixed number, $N_{c\bar{c}}$, of charm-quark pairs in the fireball for a given collision centrality,

as following from primordial production in binary N - N collisions (the underlying $c\bar{c}$ cross section is one of the main input parameters discussed in Sec. III below). For a given V_{FB} and temperature, γ_c is calculated from relative chemical equilibrium among the open- and hidden-charm states in the system, where the former are either charm hadrons in the HG phase (using vacuum masses) or charm quarks with mass $m_c^*(T)$ in the QGP phase (charmonia have a negligible impact on γ_c at the temperatures of interest here). To account for incomplete thermalization of the charm-quark spectra in the QGP, we adopt a relaxation-time approximation to correct the statistical equilibrium limit of charmonia [17]. The equilibrium limit figuring into the rate equation (1) thus takes the final form

$$N_\Psi^{\text{eq}} = \mathcal{R}(\tau) N_\Psi^{\text{stat}} , \quad \mathcal{R}(\tau) = 1 - \exp(-\tau/\tau_c^{\text{eq}}) . \quad (4)$$

The thermal relaxation time τ_c^{eq} has been taken as a fit parameter which controls the regeneration contribution in the rate equation. The resulting values, $\tau_c^{\text{eq}} \simeq 2\text{-}4$ fm/c for the WBS and SBS, respectively, are on the same order as microscopic calculations of charm-quark transport which lead to a fair description of heavy-quark observables at RHIC [18]. The impact of the \mathcal{R} -factor on the J/ψ regeneration yield at SPS and RHIC is appreciable, and quite comparable to a schematic coalescence model where the limiting cases of thermalized and initial power-law spectra have been studied [19]. Incomplete charm-quark thermalization will also play a significant role in our predictions for LHC as discussed below.

To check the equilibrium properties of charmonia against lQCD “data”, we have “reconstructed” spectral functions by combining a relativistic Breit-Wigner ansatz for the bound-state part (using $M_\Psi(T)$ and $\Gamma_\Psi(T)$ as described above, as well as a polestrength factor $Z_\Psi(T)$ to mimic the wave-function overlap at the origin) with a nonperturbative continuum (with threshold $2m_c^*(T)$). Pertinent euclidean correlator ratios turn out to be rather stable with T , deviating from 1 by ca. $\pm 10\%$ for both SBS and WBS, roughly consistent with lQCD. The vanishing of $Z_\Psi(T)$ is used to quantify the dissociation temperature, T_{diss}^Ψ , above which the gain term in the rate equation is switched off.

III. INPUT CROSS SECTIONS AT $\sqrt{s}=2760$ GEV

In this section we collect the inputs required for the initial conditions of the rate equation in the charm and charmonium sector, as well as for the thermal fireball evolution.

For the total open-charm cross section in p - p collisions at $\sqrt{s} = 5.5$ TeV recent calculations using next-to-leading order (NLO) perturbative QCD (pQCD) obtain 2.5-3.5 mb [20] using $m_c=1.5$ GeV, compared to 5-7.5 mb in earlier calculations with $m_c=1.2$ GeV [21]. Preliminary LHC data at 7 TeV [22] indicate a cross section close to the upper end of the pQCD predictions, which

is around 10 mb. Reducing this range by ca. $1/3$ - $1/2$ to extrapolate to $\sqrt{s} = 2.76$ TeV, we estimate $\sigma_{pp}^{c\bar{c}}(\sqrt{s} = 2.76 \text{ TeV}) \simeq 5$ -8 mb, in agreement with fixed-order-next-to-leading-log (FONLL) pQCD predictions [23, 24]. Converting this to a midrapidity density [21] (which amounts to dividing by a factor of 7-8 [21, 23, 24]), we arrive at $\frac{d\sigma_{pp}^{c\bar{c}}}{dy}(\sqrt{s} = 2.76 \text{ TeV}) \simeq 0.7$ -1 mb. Our calculations reported below are therefore conducted with a default value of $\frac{d\sigma_{pp}^{c\bar{c}}}{dy}(\sqrt{s} = 2.76 \text{ TeV}) = 0.75$ mb (which leads to a reasonable $(J/\psi)/(c\bar{c})$ ratio when evaluating available J/ψ cross sections, see below). The extrapolation to Pb-Pb collisions is done via standard binary-collision (N_{coll}) scaling using an inelastic p - p cross section of 65 mb accounting. At LHC energies the nuclear modification of parton distribution functions in the nucleon (shadowing) is predicted to suppress the charm cross section significantly. We will investigate this effect by performing calculations where, according to Ref. [21], the input charm cross section is reduced by up to $1/3$ for central Pb-Pb, with a centrality dependence as estimated from Refs. [25].

For the charmonium cross section p - p measurements around midrapidity are available from CDF ($\sqrt{s}=1.96$ TeV) [26] and ALICE ($\sqrt{s}=7$ TeV) [22] with $\frac{d\sigma_{pp}^{J/\psi}}{dy} = (3.4 \pm 0.3)\mu\text{b}$ and $(7.5 \pm 2)\mu\text{b}$, respectively. In addition, charm measurements at lower energies suggest an approximately constant (energy-independent) fraction of J/ψ to open-charm cross sections, $\frac{d\sigma_{pp}^{J/\psi}}{dy} / \frac{d\sigma_{pp}^{c\bar{c}}}{dy} \simeq (0.5 - 1) \%$, see, e.g., Ref. [15]. Thus we take $\frac{d\sigma_{pp}^{J/\psi}}{dy}(\sqrt{s} = 2.76 \text{ TeV}) = 4 \mu\text{b}$, which, with the above charm cross section, implies a J/ψ -to- $c\bar{c}$ fraction of 0.53%. When including charmonium shadowing in Pb-Pb we assume a suppression by $1/3$ in central collisions, consistent with recent estimates at $\sqrt{s}=5.5$ ATeV at midrapidity [27] using the color-evaporation model; this is somewhat smaller than the factor of 0.5 suppression found in Ref. [28] using EKS98 [29] or nDSg [30] shadowing, or a suppression by $2/3$ or more predicted by the Color Glass Condensate approach [31, 32]. Cold-Nuclear-Matter (CNM) effects other than shadowing are neglected. Recent empirical evaluations of the nuclear absorption cross section in p - A collisions indicate a marked reduction with increasing \sqrt{s} , suggesting it to be very small in the LHC energy regime. This is naively expected since the passage time of the nuclei at LHC has become very small. We also neglect the Cronin effect. An initial-state p_t broadening could be induced by shadowing effects which are expected to be reduced with increasing p_t , but we neglect this in the present work. It turns out that our results for the J/ψ nuclear modification factor are not sensitive to CNM effects on the J/ψ except for rather peripheral collision where the primordial component is sizable.

For the thermal medium evolution, the main empirical input is the total entropy, S , in the fireball which we assume to be conserved. We calculate the entropy density using a hadron-resonance gas equation of state (EoS)

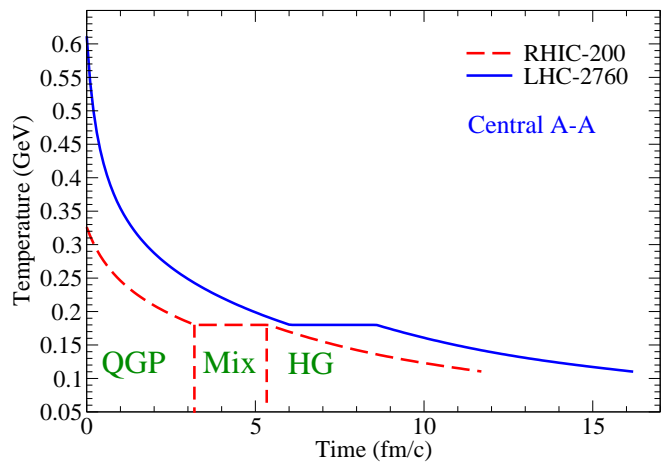


FIG. 1: (Color online) Time profile of temperature in central ($b=0$) Au-Au ($\sqrt{s}=0.2$ ATeV, $N_{\text{part}} \simeq 380$; dashed line) and Pb-Pb ($\sqrt{s}=2.76$ ATeV, $N_{\text{part}} \simeq 400$; solid line) collisions using empirical charged-hadron multiplicities, $dN_{\text{ch}}/d\eta \simeq 750$ and 1750, respectively, as input.

at chemical freezeout ($s_{\text{chem}}^{\text{HG}} \simeq 6 \text{ fm}^{-3}$ with $T_{\text{chem}} = 180$ MeV). The 3-volume is then adjusted to obtain a charged-hadron multiplicity of $dN_{\text{ch}}/d\eta \simeq 1600$ for 0-5% central Pb-Pb at $\sqrt{s}=2.76$ ATeV ($N_{\text{part}} \simeq 380$) [33], and the measured centrality dependence is employed for non-central collisions [34]. Using a QGP quasiparticle EoS for $T > T_c = T_{\text{chem}} = 180$ MeV, we connect the two phases via a first-order transition, which allows to construct the temperature evolution, $T(\tau)$, based on a cylindrical isotropic fireball volume expansion, $V_{\text{FB}}(\tau)$, using $s(T) = S/V_{\text{FB}}(\tau)$. With a formation time of $\tau_0 = 0.2 \text{ fm}/c$ the initial temperature amounts to $T_0 = 610$ MeV, compared to 330 MeV at RHIC. The lifetime of the QGP phase (where most of the J/ψ chemistry is operative) is also significantly larger, $\tau_{\text{QGP}} \simeq 6 \text{ fm}/c$ vs. $3 \text{ fm}/c$ at RHIC, see Fig. 1.

IV. CENTRALITY DEPENDENCE OF J/ψ YIELDS IN PB-PB($\sqrt{s}=2760$ GEV)

With charmonium and open-charm input cross sections, as well as the fireball evolution at each centrality fixed, we solve the rate equation (1) for the 3 charmonia $\Psi = J/\psi, \psi'$ and χ_c and obtain the final inclusive J/ψ yield using standard feeddown fractions, i.e., 32% and 8% from ψ' and χ_c in pp collisions, respectively. In addition we account for B -meson feeddown (Bfd) according to Tevatron data [26], amounting to ca. 10% of the inclusive J/ψ yield in pp (without any modifications of its p_t dependence, i.e., b -quark energy loss), see, e.g., Ref. [35]. We display the J/ψ yields in terms of the nuclear modification, either as a function of collision centrality (char-

acterized by the number of nucleon participants, N_{part}),

$$R_{AA}(N_{\text{part}}) = \frac{N_{J/\psi}(N_{\text{part}})}{N_{\text{coll}}(N_{\text{part}}) N_{J/\psi}^{pp}}, \quad (5)$$

or at fixed centrality as a function of fireball evolution time,

$$R_{AA}(\tau) = \frac{N_{J/\psi}(\tau)}{N_{\text{coll}}(N_{\text{part}}) N_{J/\psi}^{pp}}, \quad (6)$$

or transverse momentum,

$$R_{AA}(p_t) = \frac{dN_{J/\psi}/dp_t}{N_{\text{coll}}(N_{\text{part}}) dN_{J/\psi}^{pp}/dp_t}. \quad (7)$$

Let us first examine the time dependence of the exclusive J/ψ yield as a function of fireball evolution time, displayed in Fig. 2 for central Pb-Pb in the weak- and strong-binding scenario (upper and lower panel, respectively), using $\frac{\sigma_{pp}^{c\bar{c}}}{dy} = 0.75 \text{ mb}$ without shadowing. In both scenarios the large initial temperature leads to a strong and rapid suppression of the primordially produced J/ψ 's. The somewhat surprising feature is that the final regeneration yield is very similar in both scenarios, despite the different binding energies and dissociation rates at given temperature. The time dependence of the regenerated component furthermore shows that the $c\bar{c}$ coalescence occurs at rather different times or, equivalently, temperature, namely in the regime where the gain term in the rate equation first becomes operative, i.e., for $T_{\text{diss}} < 1.2(2)T_c$, corresponding to $\tau \gtrsim 4(1) \text{ fm/c}$ in the WBS (SBS). It is precisely in this regime where the dissociation (and thus formation) rate is large, facilitating a rather rapid approach of the J/ψ abundance toward its equilibrium limit. However, the “cooking” only lasts for a duration of ca. $\Delta\tau \simeq 2 - 3 \text{ fm/c}$ in both scenarios, after which the reaction rate becomes small so that the yield stabilizes.

The centrality dependence of the final J/ψ yields (including feeddown) in Pb-Pb collisions is displayed in Fig. 3, again for both WBS (upper panel) and SBS (lower panel) and for the same conditions as in the time dependence shown in Fig. 2 (i.e. N_{coll} -scaled charm cross section of $\frac{\sigma_{pp}^{c\bar{c}}}{dy} = 0.75 \text{ mb}$ without shadowing), except that bottom feeddown (Bfd) and formation-time effects (fte) are now included as detailed in Ref. [35]. One finds that the similarity of the two scenarios not only holds for central but also for semicentral and even peripheral collisions. For $N_{\text{part}} \simeq 200$ the composition of the total J/ψ yield in terms of primordial and regenerated components is quite comparable to central Au-Au collisions at RHIC, as is the charged-particle multiplicity. However, due to a smaller initial overlap volume at LHC (at identical dN_{ch}/dy) the initial temperature is significantly larger than at RHIC. In addition, charm production is larger and thus regeneration effects are more pronounced.

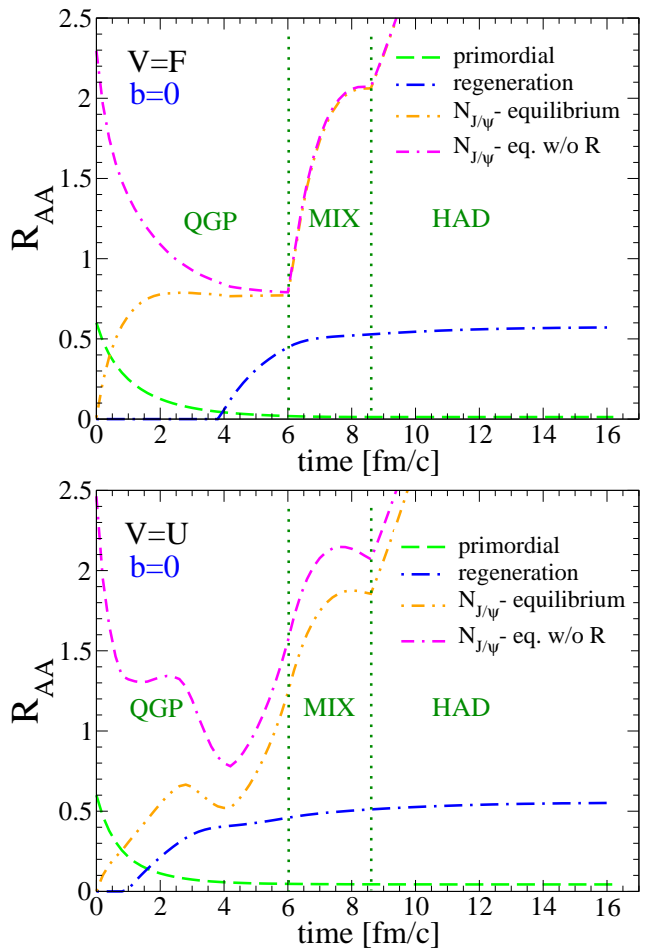


FIG. 2: (Color online) Time dependence of the J/ψ nuclear modification factor in central ($b=0$) Pb-Pb collisions at $\sqrt{s}=2.76 \text{ ATeV}$ (participant number $N_{\text{part}} \simeq 400$) at $\sqrt{s}=2.76 \text{ ATeV}$ within the WBS (top) and SBS (bottom). No shadowing effects are included; only the exclusive J/ψ contribution is included in the numerator of $R_{AA}(t)$, Eq. (6), while its denominator includes the 40% feeddown fraction, to facilitate the comparison with subsequent plots (consequently, $R_{AA}(\tau=0)=0.6$). Bottom feeddown and formation-time effects are not included.

A striking feature of our predictions is a rather large deviation of the final J/ψ yield from the values predicted by the statistical model of hadron production (upper dash-dotted lines in Fig. 3). By definition, these abundances refer to an equilibrated hadron gas at hadrochemical freezeout (which is naturally identified with the hadronization transition), with a fixed charm-quark number enforced by the fugacity, γ_c , in Eq. (3). The equilibrium limit, N_{ψ}^{eq} , in our rate equation (1) basically coincides with the statistical equilibrium limit, N_{ψ}^{stat} , since the thermal off-equilibrium \mathcal{R} -factor has become close to one at the end of the mixed phase (recall Fig. 2). While the observed light- and strange-hadron abundances in central AA collisions are in excellent agreement with the statistical model [36], our calculations suggest that the

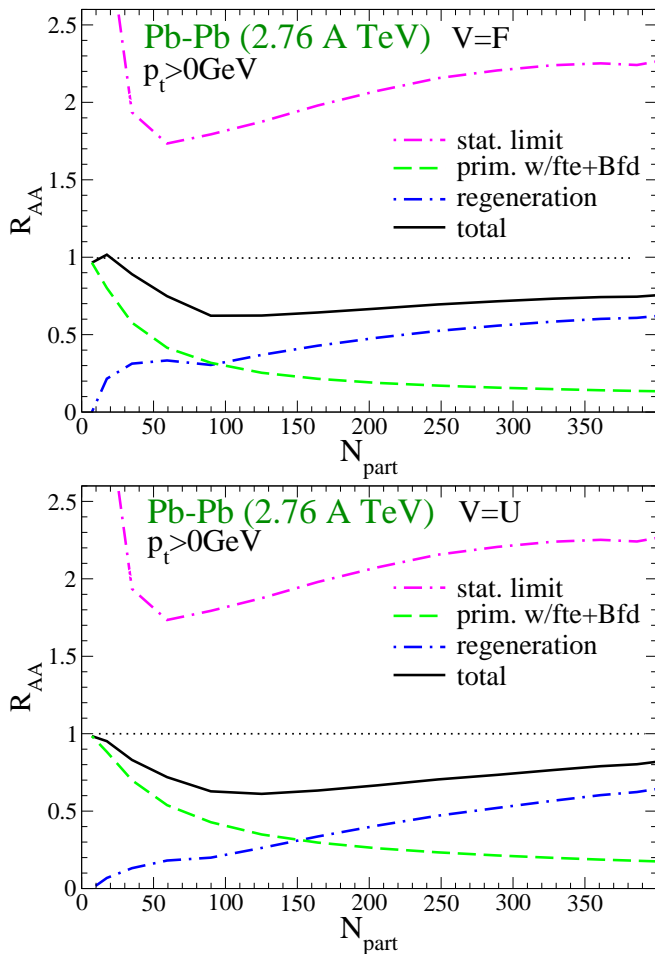


FIG. 3: (Color online) Centrality dependence of the nuclear modification factor, Eq.(5), for the inclusive J/ψ yield (including feeddown) in Pb-Pb($\sqrt{s}=2.76$ ATeV) collisions within weak- and strong-binding scenarios (upper and lower panel, respectively).

inelastic charmonium reaction rates are too small in the vicinity of T_c , especially on the hadronic side, to establish relative chemical equilibrium in the charm/onium sector. Consequently, the J/ψ yields following from the kinetic approach are well below the statistical-model limit (by about a factor of ~ 3), resulting in a suppression below one in the nuclear modification factor.

As is well known, in the grand canonical limit the equilibrium Ψ number depends quadratically on the number of open-charm pairs in the system, $N_\Psi^{\text{eq}} \propto \gamma_c^2 \propto N_{c\bar{c}}^2$. Therefore, regeneration (or statistical production) are quite sensitive to the open-charm cross section. In Fig. 4 we display our results for $R_{AA}^{J/\psi}(N_{\text{part}})$ in the SBS including a (p_t -independent) shadowing correction to both $N_{c\bar{c}}(b) = N_{\text{coll}}(b) N_{c\bar{c}}^{pp}$ and $N_\Psi(b)$, as described in Sec. III. As expected, the reduction of the $N_{c\bar{c}}$ by 1/3 in central Pb-Pb suppresses the regeneration J/ψ yield by a factor of ca. $(2/3)^2 \simeq 1/2$, so that the total R_{AA} decreases from ~ 0.8 to 0.45 (no shadowing is applied to the bot-

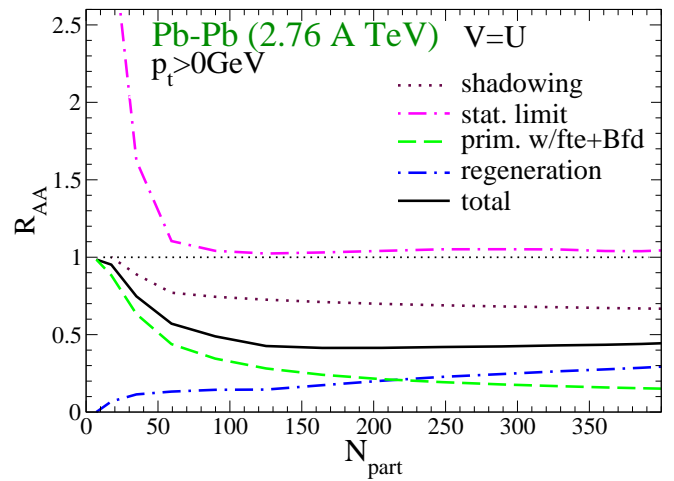


FIG. 4: (Color online) Nuclear modification factor for the inclusive J/ψ yield (including feeddown) in Pb-Pb($\sqrt{s}=2.76$ ATeV) collisions within the strong-binding scenario including a shadowing correction of the N_{coll} -scaled open-charm and J/ψ cross sections by a factor of 2/3 for $N_{\text{part}} \simeq 400$.

tom feeddown contribution). This underlines again the importance of an accurate open-charm input cross section for in-medium charmonium physics at LHC.

Next, we investigate the transverse-momentum spectra of inclusive J/ψ production, displayed in Fig. 5 for peripheral and central Pb-Pb collisions (upper and lower panel, respectively). For simplicity we restrict ourselves to predictions without shadowing corrections. At both centralities the regeneration yield generates a marked enhancement of the spectra at low p_t . The maximum structure is more pronounced in central collisions due to larger regeneration and larger suppression of the primordial production; the crossing between the two components occurs at $p_t \simeq 5-6$ GeV, compared to $p_t \simeq 0$ GeV for peripheral collisions. The latter is reminiscent of central Au-Au collisions in the SBS at RHIC [12], although there no significant maximum develops at low p_t (the charm cross section is too small and the suppression of the primordial component is stronger in central Au-Au($\sqrt{s}=0.2$ ATeV) than in peripheral Pb-Pb($\sqrt{s}=2.76$ ATeV). We note, however, that shadowing corrections are expected to be most pronounced at low p_t (i.e., small values of $x = 2p_t/\sqrt{s}$ at midrapidity) and fade away at high p_t . Since shadowing suppresses both regeneration and primordial production, our calculations in Fig. 5 may be viewed as an upper limit for the maximum at low p_t .

Finally, we perform a calculation for the so-called central-to-peripheral ratio of J/ψ mesons, which is similar to R_{AA} but normalized to a peripheral centrality bin,

$$R_{CP}(N_{\text{part}}) = \frac{N_\psi(N_{\text{part}})/N_{\text{coll}}(N_{\text{part}})}{N_\psi^{\text{peri}}/N_{\text{coll}}^{\text{peri}}} . \quad (8)$$

A first measurement of this quantity in Pb-Pb at LHC

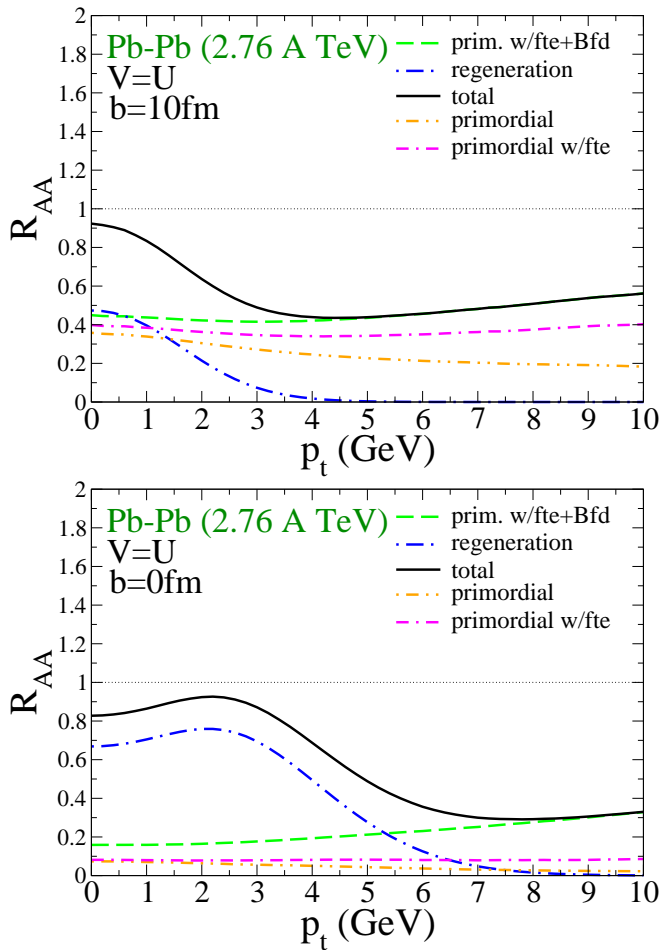


FIG. 5: (Color online) Transverse-momentum dependence of the nuclear modification factor, Eq.(7), for inclusive J/ψ 's (including feeddown) in peripheral (upper panel) and central (lower panel) Pb-Pb ($\sqrt{s}=2.76$ ATeV) collisions within the strong-binding scenario (no shadowing corrections accounted for).

has recently been reported by the ATLAS collaboration [37] where the peripheral bin corresponds to a 40-80% centrality selection. In addition, only muons with $p_t^\mu > 3$ GeV were accepted, implying that ca. 80% of the reconstructed J/ψ carry a transverse momentum of $p_t > 6.5$ GeV. We mimic these conditions in our calculation by representing the 40-80% centrality bin with an average $N_{\text{part}} \simeq 40$ and using a momentum cut of $p_t > 6.5$ GeV for all J/ψ 's (neglecting shadowing). The latter implies that the regeneration contribution is essentially gone, recall Fig. 5 so that our calculated R_{CP} only involves primordially (suppressed) J/ψ 's, including bottom feeddown and formation-time effects in the QGP suppression reactions [35]. The trend of our postdiction (without any adjustment of parameters) is fairly compatible with the ATLAS measurement, cf. Fig. 6. We emphasize again that the high- p_t cut evades conclusions about regeneration mechanism other than that they are not operative in this regime.

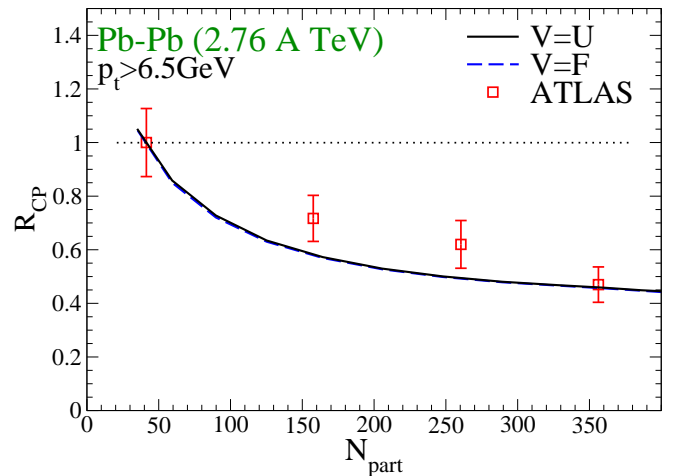


FIG. 6: (Color online) Central-to-peripheral ratio, R_{CP} , for inclusive J/ψ yields (including feeddown) in Pb-Pb ($\sqrt{s}=2.76$ ATeV) collisions within the strong- and weak-binding scenario (solid and dashed line, respectively; no shadowing included). A $p_t > 6.5$ GeV cut has been applied to all J/ψ 's in the calculations to compare to ATLAS data [37].

V. CONCLUSION

Employing a kinetic rate-equation approach which incorporates in-medium effects extracted from charmonium spectral functions we have computed inclusive J/ψ production in Pb-Pb collisions as recently conducted at the LHC. Our approach reproduces existing charmonium data at SPS and RHIC energies where the two main model parameters had been adjusted (strong coupling constant in the dissociation rate and thermal off-equilibrium correction in the equilibrium limit). Our pertinent predictions for LHC indicate a large suppression of primordial charmonia (by a factor of ~ 10 in central Pb-Pb) and thus a predominance of the regeneration yield for participant numbers $N_{\text{part}} > 100 - 150$. However, the final yield stays well below the predictions of the statistical model, by about a factor of ~ 3 , implying an $R_{AA}^{J/\psi}$ below one even for an input charm cross section of 0.75 mb in pp collisions; shadowing corrections on this quantity further suppress the final J/ψ yield. Somewhat surprisingly, both strong- and weak-binding scenarios give very similar results, which we attribute to the rather limited time window ($\Delta\tau \simeq 2 - 3$ fm/c) during which the gain term in the rate equation is active (below T_{diss}) and the inelastic reaction rate is large. In the strong-binding scenario J/ψ 's form at significantly higher temperatures and thus at earlier times in the fireball evolution than for weak binding. This may lead to discernible differences in the finally observed elliptic flow, which, however, will have to be measured with rather good precision. We also performed calculations of $R_{CP}^{J/\psi}$ in comparison to very recent ATLAS data, finding a suppression roughly compatible with experiment. However, due to the large- p_t cut in these data ($p_t > 6.5$ GeV), our result is not sensitive to regeneration

contributions which only figure at lower $p_t \lesssim 6(3)$ GeV for central (peripheral) collisions. Upcoming LHC data are eagerly awaited to test our predictions and give further insights into charmonium production mechanisms in hot/dense QCD matter.

Acknowledgments

We thank A. Andronic, M. Cacciari, E. Musto, J. Schukraft and K. Tuchin for valuable discussions.

This work is supported by the US National Science Foundation under grant no. PHY-0969394 (RR, XZ), by the A.-v.-Humboldt foundation (RR) and by the US Department of Energy under grant no. DE-FG02-87ER40371 (XZ).

-
- [1] T. Matsui and H. Satz, Phys. Lett. B **178**, 416 (1986).
 - [2] R. Rapp, D. Blaschke and P. Crochet, Prog. Part. Nucl. Phys. **65**, 209 (2010).
 - [3] L. Kluberg and H. Satz, arXiv:0901.3831 [hep-ph].
 - [4] P. Braun-Munzinger and J. Stachel, arXiv:0901.2500 [nucl-th].
 - [5] L. Grandchamp, R. Rapp and G.E. Brown, Phys. Rev. Lett. **92**, 212301 (2004).
 - [6] R.L. Thews and M.L. Mangano, Phys. Rev. C **73**, 014904 (2006).
 - [7] L. Yan, P. Zhuang and N. Xu, Phys. Rev. Lett. **97**, 232301 (2006).
 - [8] X. Zhao and R. Rapp, Phys. Lett. B **664**, 253 (2008).
 - [9] C. Young and E. Shuryak, Phys. Rev. C **79**, 034907 (2009).
 - [10] O. Linnyk, E. L. Bratkovskaya and W. Cassing, Nucl. Phys. A **807**, 79 (2008).
 - [11] T. Song, C.M. Ko, S.H. Lee and J. Xu, arXiv:1008.2730 [hep-ph].
 - [12] X. Zhao and R. Rapp, Phys. Rev. C **82**, 064905 (2010).
 - [13] F. Riek and R. Rapp, Phys. Rev. C **82**, 035201 (2010).
 - [14] L. Grandchamp and R. Rapp, Phys. Lett. B **523**, 60 (2001).
 - [15] A. Andronic, P. Braun-Munzinger, K. Redlich and J. Stachel, Nucl. Phys. A **789**, 334 (2007).
 - [16] A. Andronic, P. Braun-Munzinger, K. Redlich and J. Stachel, J. Phys. G **37**, 094014 (2010).
 - [17] L. Grandchamp and R. Rapp, Nucl. Phys. A **709**, 415 (2002).
 - [18] H. van Hees, M. Mannarelli, V. Greco and R. Rapp, Phys. Rev. Lett. **100**, 192301 (2008).
 - [19] V. Greco, C. M. Ko and R. Rapp, Phys. Lett. B **595**, 202 (2004).
 - [20] R. Vogt, Eur. Phys. J. C **61**, 793 (2009).
 - [21] M. Bedjidian *et al.*, arXiv:hep-ph/0311048.
 - [22] A. Dainese *et al.* [ALICE Collaboration], arXiv:1012.4036 [hep-ex].
 - [23] M. Cacciari, priv. comm. (2011).
 - [24] M. Cacciari, P. Nason and R. Vogt, Phys. Rev. Lett. **95**, 122001 (2005).
 - [25] K. Tuchin, Nucl. Phys. A **798**, 61 (2008); and priv. comm. (2011).
 - [26] D. Acosta *et al.* [CDF Collaboration], Phys. Rev. D **71**, 032001 (2005).
 - [27] R. Vogt, Phys. Rev. C **81**, 044903 (2010).
 - [28] N. Armesto *et al.*, J. Phys. G **35**, 054001 (2008).
 - [29] K.J. Eskola, V.J. Kolhinen, C.A. Salgado, Eur. Phys. J. **C9**, 61-68 (1999).
 - [30] D. de Florian and R. Sassot, Phys. Rev. D **69**, 074028 (2004).
 - [31] K. Tuchin, arXiv:1012.4212 [hep-ph].
 - [32] D. Kharzeev, E. Levin, M. Nardi and K. Tuchin, Phys. Rev. Lett. **102**, 152301 (2009).
 - [33] K. Aamodt *et al.* [The ALICE Collaboration], Phys. Rev. Lett. **105**, 252301 (2010).
 - [34] K. Aamodt *et al.* [ALICE Collaboration], Phys. Rev. Lett. **106**, 032301 (2011).
 - [35] X. Zhao and R. Rapp, arXiv:0806.1239 [nucl-th].
 - [36] P. Braun-Munzinger, K. Redlich and J. Stachel, arXiv:nucl-th/0304013.
 - [37] G. Aad *et al.* [The ATLAS Collaboration], arXiv:1012.5419 [hep-ex].